Available online at www.sciencedirect.com
SCIENCE DIRECT®
Journal of Nuclear Materials 342 (2005) 63–67
journal of nuclear materials
www.elsevier.com/locate/jnucmat

Beryllium–tungsten mixed-material interactions

R.P. Doerner [a,*], M.J. Baldwin [a], R.A. Causey [b]

[a] University of California at San Diego, La Jolla, CA 92093-0417, USA
[b] Sandia National Laboratory, Livermore, CA 94550, USA

Received 14 January 2005; accepted 1 March 2005

Abstract

A beryllium-seeded deuterium plasma is used to investigate beryllium–tungsten mixed-material properties. Beryllium accumulation on tungsten surfaces exposed to deuterium plasma containing only a small beryllium impurity concentration (0.1%) is observed. The beryllium seeding oven utilizes a tungsten crucible to hold the hot beryllium. This crucible destructively melted after only 100 h of operation and at temperatures that never exceeded 1550 °C. A tungsten–beryllide alloy appears to have formed in the melt zone of the tungsten crucible.

PACS: 52.40.Hf

1. Introduction

The present ITER design [1] employs beryllium tiles as the first wall plasma-facing material. In the divertor area, a combination of tungsten tiles and carbon–fiber composites form the plasma facing materials. The Joint European Torus (JET) is also entertaining the idea of investigating issues related to the use of the ITER materials by installing a full beryllium wall experiment. In the JET design the divertor will be composed of either of a combination of tungsten and carbon (as in ITER), or entirely of tungsten surfaces. Understanding the behavior of a mixed beryllium–tungsten surface will be critical to the success of these two large new experimental endeavors.

A beryllium-seeded deuterium plasma is used in PISCES-B to investigate mixed-material erosion and redeposition properties of ITER relevant divertor materials. The beryllium containing plasma simulates the erosion of first wall material into the ITER sol plasma and its subsequent flow toward the carbon and tungsten material located in the divertor region. The PISCES-B device [2,3] has been modified by adding a commercial high-temperature effusion cell from Veeco Applied EPI, in order to seed a controllable amount of beryllium impurities into the plasma column, to accomplish this experimental program. The orientation of the atom beam emerging from this oven is such that the beam travels perpendicular to the magnetic axis of PISCES-B. Due to the rather slow thermal velocity of the Be atoms, some amount of the beam of atoms is attenuated in the plasma column due to ionization [2]. The beryllium ions are then entrained in the plasma flow toward the target. A schematic of the experimental setup is shown in Fig. 1. The concentration of beryllium ions within the plasma column is measured by observing the BeII line emission at 467 nm and can be controlled by varying the temperature of the oven. Ionization and

* Corresponding author. Tel.: +858 534 7830.
E-mail address: rdoerner@ucsd.edu (R.P. Doerner).

0022-3115/$ - see front matter © 2005 Elsevier B.V. All rights reserved.
doi:10.1016/j.jnucmat.2005.03.016

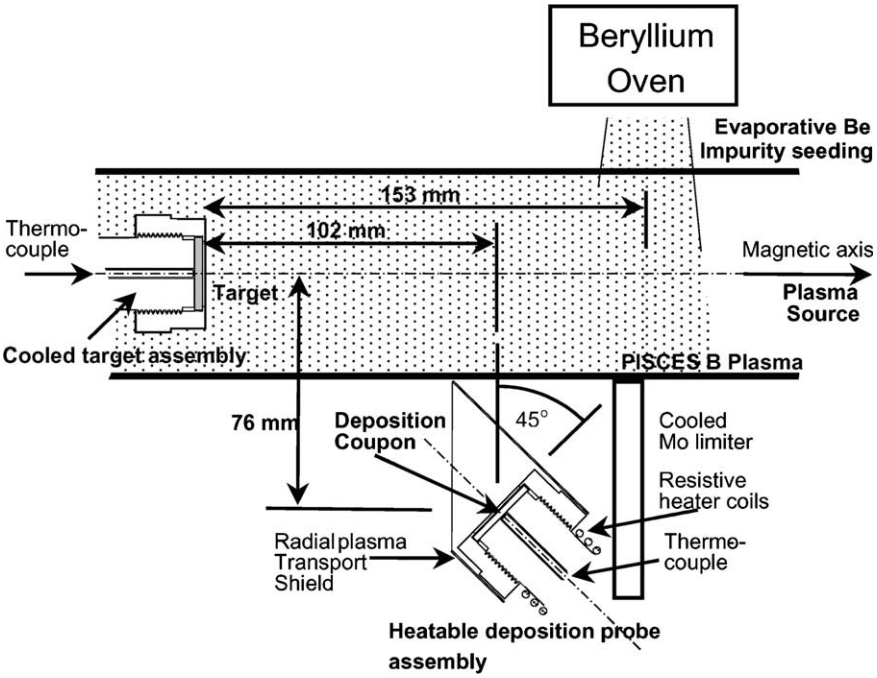

Fig. 1. Schematic drawing showing arrangement of PISCES-B beryllium seeding experiments.

excitation rate coefficients were obtained from the ADAS data base [4]. The beryllium ionization rates have previously been experimentally verified in PISCES-B [5].

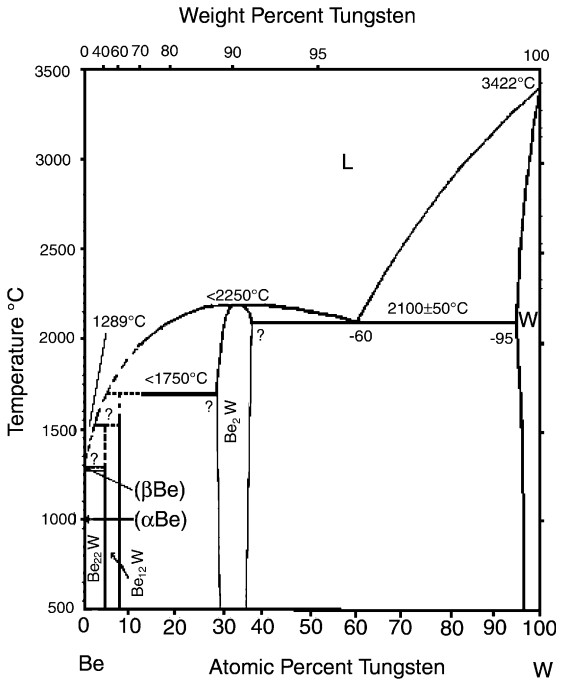

Fig. 2. Tungsten–beryllium phase diagram reproduced from [10].

The present PISCES-B experiments are focused on investigating the interaction between tungsten samples and a beryllium-seeded deuterium plasma, similar to Be–C interaction experiments reported previously [6]. Be–W alloy formation has been observed and reported in the literature [7–9]. Fig. 2 shows the beryllium–tungsten phase diagram (reproduced from [10]). Of particular importance in this diagram is the beryllium rich end of the phase diagram. The alloys $Be_{22}W$, $Be_{12}W$ and Be_2W, all exhibit some degree of reduced melting temperature compared to pure tungsten.

2. Results from Be–W interaction experiments

A systematic investigation of beryllium-seeded deuterium plasma interactions with carbon surfaces has previously been reported [11]. Here the identical experimental technique is used to examine the behavior of tungsten samples exposed to a beryllium containing deuterium plasma. As was seen during the carbon sample experiments [6], a beryllium rich coating also forms on the tungsten samples during very low levels of beryllium seeding of the plasma column. Fig. 3 shows an Auger electron spectroscopy (AES) depth profile of the surface of a tungsten sample exposed to deuterium plasma containing 0.1% beryllium impurity ions (for reference ITER expects 1–10% beryllium impurity fraction in the divertor plasma). This sample was exposed for 5000 s to deuterium plasma at a flux of $1 \times 10^{18}\ cm^{-2}\ s^{-1}$. An

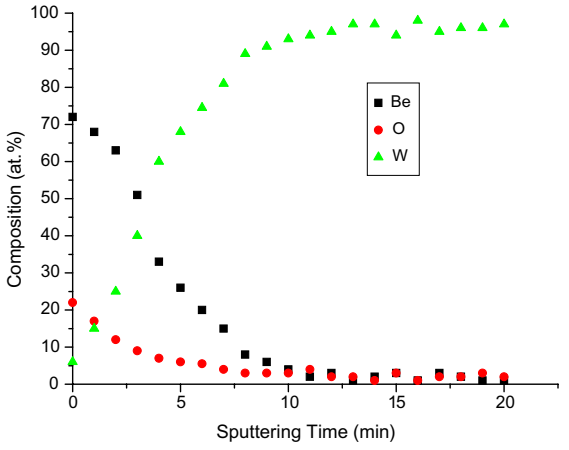

Fig. 3. Elemental composition of a tungsten target plate exposed to a 0.1% beryllium containing deuterium plasma.

incident ion energy of approximately 75 eV was obtained by biasing the tungsten sample holder to −75 V. The temperature of the tungsten sample during the exposure was 300 °C. The sputtering time of 3 min in the AES profile corresponds to roughly 10 nm. The stopping distance of a 75 eV beryllium ion in tungsten is less than 1 nm. A beryllium rich surface layer which is much thicker than the implantation zone results from the plasma exposure. The surface layer contains about 12 times as much beryllium at the surface compared to tungsten.

The data relating to equilibrium Be–W interactions shows that the $Be_{12}W$ alloy begins to form at a temperature of around 750 °C and that the $Be_{22}W$ alloy forms at around 980 °C [7]. However, it has been shown experimentally that chemical reactions occur during non-equilibrium energetic particle bombardment of surfaces at temperatures much below their equilibrium values [12,13]. Additionally, it has been shown [9] that the Be–W reaction rate is kinetics controlled, rather than diffusion controlled, and therefore the interaction zone propagates as a wave front through the material.

The number of beryllium atoms composing the surface layer is much less than the total number of incident beryllium ions in the plasma column. The total fluence of beryllium ions was 5×10^{18} cm^{-2}, whereas the number of beryllium atoms remaining in the 10 nm thick surface layer of the tungsten sample is approximately 1.2×10^{17} cm^{-2}. This indicates that the surface reaction between the beryllium and tungsten is not limited by the amount of beryllium available. While there is no data available on the nature of the Be–W bonding in Fig. 3, one can still estimate a growth rate of the Be–W layer. In the case of the sample shown in Fig. 3, one obtains a growth rate of the Be–W alloy of 2×10^{-10} cm/s (i.e. 10^{-6} cm in 5000 s at 300 °C). This value can be compared to equilibrium growth rate data for tungsten–beryllide alloys found in the literature [9] and shown in Fig. 4. The fact that the growth rate of the layer is much faster during plasma bombardment is due to the non-equilibrium nature of the surface during the bombardment. Beryllium ions are being implanted into the tungsten surface causing damage to the tungsten lattice and allowing tungsten–beryllides to form more quickly at low temperature.

Some additional qualitative insight into the importance of Be–W alloys can be gained from the PISCES-B experiments as the effusion cell used in the beryllium seeding oven during these experiments utilized a tungsten crucible to hold the high temperature beryllium ingot used to add beryllium impurities to the deuterium plasma. The tungsten crucible used in PISCES-B suffered destructive melting after only about 100 h of beryllium seeding operations. While the temperature of the tungsten crucible varied from day to day, its maximum operating temperature never exceeded 1550 °C. The actual failure of the crucible occurred during operation at only 1200 °C.

If one assumes that the majority of the Be–W interaction occurred when the oven was operating in its highest temperature region (i.e. between 1450 °C and 1550 °C), then it is possible to estimate the growth rate of the Be–W region. The original crucible wall thickness was 0.07 cm and the oven operated in the high temperature region for a total of about 25 h. This corresponds to a growth rate of approximately 8×10^{-6} cm/s at about 1500 °C. This growth rate seems to fit in with the other tungsten–beryllide growth rate data [9] shown in Fig. 4.

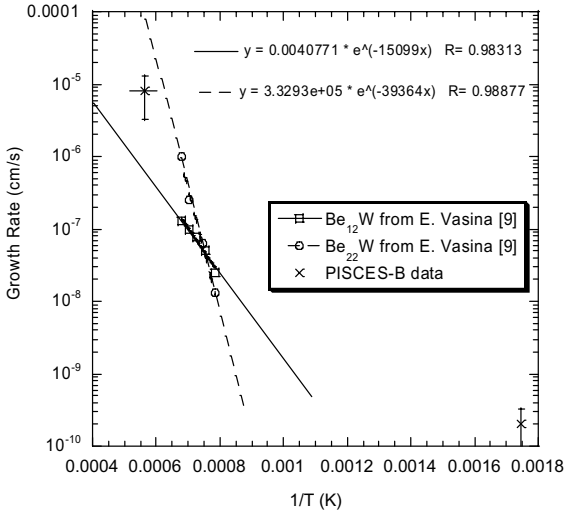

Fig. 4. Estimated growth rate of tungsten–beryllide as a function of temperature.

Fragments of the disintegrated crucible have been analyzed using an Oxford Instruments wavelength dispersive spectroscopy (WDS) system attached to a JEOL scanning electron microscope. Two images are shown in Fig. 5. Fig. 5(a) shows a fragment of an intact region of the tungsten crucible wall. In this region a thin beryllium rich layer (250–300 μm thick) containing approximately 4% tungsten is observed to cover the inner wall of the tungsten crucible. This concentration is consistent with the $Be_{22}W$ alloy. The pure tungsten wall section appears to be about 400 μm thick. In this section of the crucible wall it appears that the tungsten–beryllide layer is slowly migrating though the wall of the crucible. This region of the crucible would have come into contact with only beryllium vapor from the hot beryllium ingot located in a different part of the crucible.

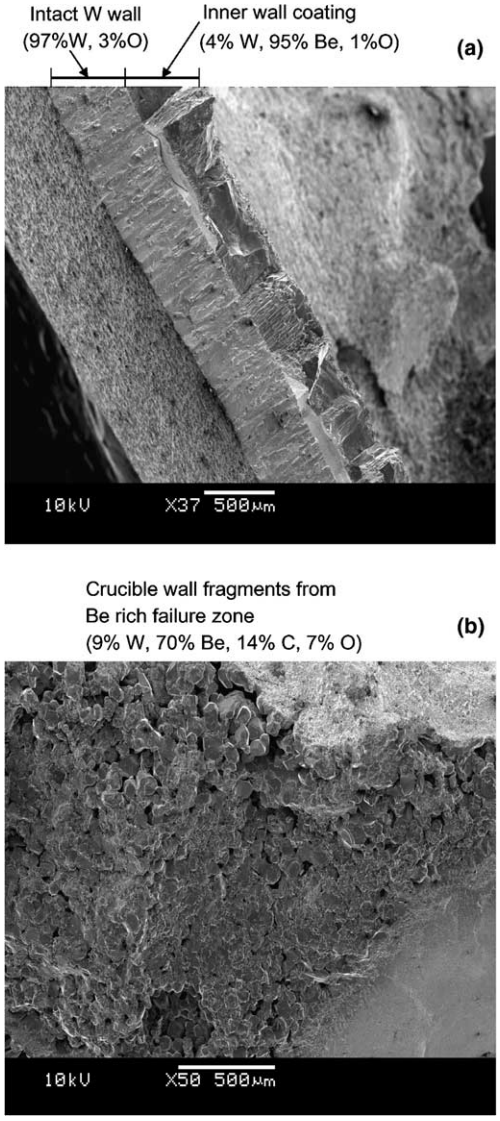

Fig. 5. (a) Cross-section of the tungsten crucible showing a Be–W material coating on the inner wall of the crucible in the region that did not melt. (b) An image of a crucible remnant from the crucible melt zone.

Fig. 5(b) shows a similar image of a section of the tungsten crucible from the failure region. The failure region is in the location where the hot beryllium ingot was located. Clearly, a much different, nodular structure appears in this region. The nodular structure appears to be resolidified material and is extremely fragile to touch. The quantitative compositional analysis reveals 9%W distributed in a beryllium rich material extending throughout the remnants of the crucible wall. This composition is similar to the $Be_{12}W$ alloy represented in the Be–W phase diagram. Our interpretation is that in this region the crucible wall was in direct contact with the hot/molten beryllium ingot and as such the tungsten–beryllide formation reaction was not restricted by the amount of beryllium available. Once the tungsten–beryllide formed across the thickness of the crucible wall, the crucible either melted or sagged under its own weight, resulting in contact with the heater assembly of the oven. The observed $Be_{12}W$ alloy may have formed originally in the region, or it is more likely that the $Be_{22}W$ alloy formed (because this phase is favored at elevated temperature [7]) and subsequently melted, resulting in the formation of the $Be_{12}W$ alloy and beryllium-rich liquid, which subsequently vaporized (see the Be–W phase diagram, Fig. 2).

3. Discussion

Recent measurements in PISCES-B have clearly shown that beryllium–tungsten interactions can be a serious concern. However, it is not clear whether, or to what extent, such reactions will be a critical issue for the plasma-facing surfaces in the ITER device. It is possible that the high surface temperature encountered in ITER's tungsten baffle region will result in rapid sublimation of any beryllium incident on these surfaces. This rate limiting effect appears to have been observed during static heating tests of beryllium coated tungsten test pieces [14]. If the amount of surface beryllium is limited, either due to the incident flux of beryllium, or due to the loss rate of beryllium from the tungsten surface, then the growth rates of tungsten–beryllides will also be limited.

If on the other hand, there is a sufficient flux of incident beryllium available from the first wall region, the reaction rate of beryllium and tungsten is quite rapid. The impact of the formation of tungsten–beryllide surfaces is largely an unknown. While it is clear that such alloys have reduced melting temperature, little else is known of their properties. The thermal conductivity, tritium retention and release characteristics, thermal shock

behavior, etc., all must be measured and investigated before any definitive conclusions on the impact on ITER can be determined.

Acknowledgements

This work was performed as part of a US-EU Collaboration on Mixed-Material Plasma Material Interactions. Support for this research from both the US DOE and EFDA are gratefully acknowledged. In addition, the support of the PISCES-B beryllium team (of which T. Lynch played a major role) was instrumental in this successful experimental endeavor. We are pleased to have the opportunity to acknowledge their expertise.

References

[1] G. Federici, P. Andrew, P. Barabaschi, et al., J. Nucl. Mater. 313–316 (2003) 11.
[2] R.P. Doerner, M.J. Baldwin, K. Schmid, Phys. Scr. T 111 (2004) 75.
[3] D.G. Whyte, G. Tynan, R.P. Doerner, J.N. Brooks, Nucl. Fus. 41 (2001) 47.
[4] H.P. Summers, Atomic Data and Analysis Structure – User Manual, Rep. JET-IR(94), JET Joint Undertaking, Abingdon, 1994.
[5] R.P. Doerner, D.G. Whyte, D.M. Goebel, J. Appl. Phys. 93 (2003) 5816.
[6] K. Schmid, M. Baldwin, R. Doerner, A. Wiltner, Nucl. Fus. 44 (2004) 815.
[7] C.R. Watts, Int. J. Powder Met. 4 (1968) 49.
[8] A.S. Panov, M.M. Rysina, Russ. Metall. (Metally) 1 (1970) 133.
[9] E.A. Vasina, A.S. Panov, Russ. Metall. (Metally) 1 (1974) 119.
[10] H. Okamoto, L.E. Tanner, in: S.V. Nagendra Naidu, P. Ramo Rao (Eds.), Phase Diagrams of Binary Tungsten Alloys, Indian Institute of Metals, Calcutta, 1991.
[11] K. Schmid, M. Baldwin, R. Doerner, J. Nucl. Mater. 337–339 (2005) 862.
[12] P. Goldstrass, Ch. Linsmeier, J. Nucl. Mater. 290–293 (2001) 71.
[13] R.P. Doerner, S.C. Luckhardt, R. Seraydarian, F.C. Sze, D.G. Whyte, Phys. Scr. T 81 (1999) 35.
[14] A. Wiltner, Ch. Linsmeier, J. Nucl. Mater. 337–339 (2005) 951.